Pten Deficiency in Melanocytes Results in Resistance to Hair Graying and Susceptibility to Carcinogen-Induced Melanomagenesis

Tae Inoue-Narita,[1] Koichi Hamada,[2,4] Takehiko Sasaki,[3] Sachiko Hatakeyama,[1] Sachiko Fujita,[1] Kohichi Kawahara,[2,4] Masato Sasaki,[2] Hiroyuki Kishimoto,[2] Satoshi Eguchi,[3] Itaru Kojima,[5] Friedrich Beermann,[6] Tetsunori Kimura,[7] Masatake Osawa,[8] Satoshi Itami,[9] Tak Wah Mak,[11] Toru Nakano,[10] Motomu Manabe,[1] and Akira Suzuki[2,4]

Departments of [1]Dermatology, [2]Molecular Biology, and [3]Microbiology, Akita University School of Medicine, Akita, Japan; [4]Division of Embryonic and Genetic Engineering, Medical Institute of Bioregulation, Kyushu University, Fukuoka, Japan; [5]Laboratory of Cell Physiology, Institute for Molecular and Cellular Regulation, Gunma University, Maebashi, Japan; [6]Swiss Institute for Experimental Cancer Research (ISREC), School of Life Sciences, Ecole Polytechnique Féderale de Lausanne (EPFL), Epalinges, Switzerland; [7]Sapporo Institute of Dermatopathology, Sapporo, Japan; [8]Cutaneous Biology Research Center, Massachusetts General Hospital, Harvard Medical School, Charlestown, Massachusetts; Departments of [9]Regenerative Dermatology and [10]Pathology, Graduate School of Medicine, Osaka University, Suita, Japan; and [11]The Campbell Family Institute for Breast Cancer Research and Departments of Immunology and Medical Biophysics, University of Toronto, Toronto, Ontario, Canada

Abstract

Phosphate and tensin homologue deleted on chromosome 10 (*PTEN*) is a tumor suppressor gene inactivated in numerous sporadic cancers, including melanomas. To analyze *Pten* functions in melanocytes, we used the *Cre-loxP* system to delete Pten specifically in murine pigment-producing cells and generated *DctCrePten*$^{flox/flox}$ mice. Half of *DctCrePten*$^{flox/flox}$ mice died shortly after birth with enlargements of the cerebral cortex and hippocampus. Melanocytes were increased in the dermis of perinatal *DctCrePten*$^{flox/flox}$ mice. When the mutants were subjected to repeated depilations, melanocyte stem cells in the bulge of the hair follicle resisted exhaustion and the mice were protected against hair graying. Although spontaneous melanomas did not form in *DctCrePten*$^{flox/flox}$ mice, large nevi and melanomas developed after carcinogen exposure. *DctCrePten*$^{flox/flox}$ melanocytes were increased in size and exhibited heightened activation of Akt and extracellular signal–regulated kinases, increased expression of Bcl-2, and decreased expression of p27^{Kip1}. Our results show that *Pten* is important for the maintenance of melanocyte stem cells and the suppression of melanomagenesis. [Cancer Res 2008;68(14):5760–8]

Introduction

Melanocytes produce the pigment melanin that governs hair color. Melanocytes in the hair follicles arise from melanoblasts that originate in the embryonic neural crest. After birth, hair regeneration initiates at the early anagen stage in the bulge area of the follicle, where stem cells that give rise to follicular keratinocytes reside (1). Within the basal portion of the hair follicles, the hair matrix, composed of keratinocytes and melanocytes, grows downward during anagen. During catagen, the hair follicles regress and become resting at the telogen stage. The cyclical nature of the hair follicle also influences the life cycle of a melanocyte. Melanocyte stem cells (MSC), which are slow-cycling cells capable of both self-renewal and differentiation into mature melanocytes, are localized in the bulge area (2). When a MSC divides, at least one stem cell remains in the bulge while the other daughter stem cells migrate into the hair matrix and terminally differentiate into melanin-producing follicular melanocytes. Once a follicular melanocyte transfers pigment granules to keratinocytes in the hair matrix during anagen, the melanocytes die by apoptosis during catagen (3).

Hair graying is the most obvious sign of human aging, and much cosmetic research is focused on preventing this rite of passage. Hair graying is caused by defective self-maintenance of MSCs (4). Bcl-2 may protect MSCs from apoptosis, as the coats of Bcl-2$^{-/-}$ mice turn gray during the second hair follicle cycle (5). In addition, mutations in genes that are critical for melanocyte development, such as microphthalmia-associated transcription factor (*Mitf*), *Pax3*, the Notch pathway, and *Kit*, impair hair pigmentation. Similarly, mutations in C57BL/6 mice of melanin production enzymes such as tyrosinase, tyrosinase-related protein 1 (Trp1), and dopachrome tautomerase [Dct; also called tyrosinase-related protein 2 (Trp2)] result in either albino mice (tyrosinase mutations) or brown mice (Trp1 and Dct mutations; ref. 6). However, most of the >120 genes known to influence murine coat color are unknown (6).

Malignant melanoma is the most significant and potentially lethal human skin cancer. Both the incidence of melanoma and its associated mortality rate are increasing, and there is currently no effective long-term treatment. Because the genes altered during melanomagenesis are unknown, it has been difficult to design targeted therapies to treat this tumor (7).

Phosphate and tensin homologue deleted on chromosome 10 (*PTEN*) is a tumor suppressor gene that is mutated in many human sporadic cancers and in hereditary tumor susceptibility disorders such as Cowden disease (8). PTEN is a multifunctional phosphatase whose major substrate is phosphatidylinositol-3,4,5-triphosphate (PIP3; ref. 9). PIP3 activates numerous downstream targets including the serine-threonine kinase Akt, which is involved in antiapoptosis, proliferation, and oncogenesis. PTEN uses its lipid phosphatase activity to dephosphorylate PIP3 and negatively regulate the Akt pathway, thus exerting tumor suppression. PIP3 is generated by phosphoinositide-3-kinases (PI3K), which are activated by a wide range of growth factors. PTEN uses its protein

Note: Supplementary data for this article are available at Cancer Research Online (http://cancerres.aacrjournals.org/).

M. Manabe and A. Suzuki contributed equally to this work as last authors.

Requests for reprints: Akira Suzuki, Division of Embryonic and Genetic Engineering, Medical Institute of Bioregulation, Kyushu University, Maidashi 3-1-1, Higashi-ku, Fukuoka, Fukuoka 812-8582, Japan. Phone: 81-92-642-6838, Fax: 81-92-632-1499; E-mail: suzuki@bioreg.kyushu-u.ac.jp.

doi:10.1158/0008-5472.CAN-08-0889

phosphatase activity to inactivate focal adhesion kinase, Shc, and platelet-derived growth factor receptor. The inactivation of these molecules shuts down the extracellular signal–regulated kinase (Erk) pathway, inhibiting cell invasion, migration, and growth (10).

Mutations of PTEN or loss of heterozygosity at the *PTEN* locus occurs at relatively low frequency in primary melanomas (<15% and 0–50%, respectively; ref. 11) and in melanoma cell lines (9–30% and 20–50%, respectively). However, absent or decreased PTEN protein expression occurs in 50% to 91% of primary melanomas (12). Indeed, ectopic expression of PTEN in a PTEN-deficient melanoma cell line reduced melanoma formation and metastasis (13). Akt3 is activated in 43% to 60% of sporadic melanomas (14), perhaps explaining why PTEN-null melanoma cells showed a growth advantage in a murine transplant model (15). However, it is unclear whether loss of PTEN alone can induce melanomagenesis *in vivo*.

Here, we analyze Pten functions in melanocytes *in vivo* by characterizing mice with a conditional *Pten* mutation in pigment-producing cells. We show that Pten protects against hair graying by preventing MSC exhaustion and that Pten suppresses carcinogen-induced melanoma formation.

Materials and Methods

Generation of mice bearing Pten-deficient melanocytes and PCR analysis of Pten genotypes. For a detailed discussion, see Supplementary data.

Preparation and *in vitro* culture of melanocytes. Melanocyte cultures were established as described (16) with modifications. Briefly, full-thickness dorsal skin obtained from newborn mice was treated with 500 units/mL dispase (Godo Shusei) overnight at 4°C. Epidermal sheets were dissociated using trypsin-EDTA, and cells (1×10^6 per dish) were plated in 35-mm polystyrene dishes precoated with type I collagen (Nitta Gelatin). Cells were cultured for 14 d in melanocyte-defined medium supplemented with 0.5 mmol/L DB-cAMP and 10 nmol/L endothelin-1 (all from Sigma). Cultured melanocytes were >92% pure as assessed by anti-Dct staining.

Western blots. Aliquots (10–30 μg) of total lysates of cultured melanocytes or tumor tissues were analyzed by standard Western blotting as described (17). Antibodies used were directed against Pten (Cascade Biosciences); actin, β-catenin, $p16^{Ink4a}$, $p21^{cip/waf1}$, p53, Bcl-2, c-Kit, Notch1, tyrosinase, Trp1, or Dct (Trp2; all from Santa Cruz); phospho-Akt/PKB(Ser^{473}), total Akt, phospho-Erk1/2(Thr^{202}/Tyr^{204}), and total Erk1/2 (all from Cell Signaling Technology); $p19^{Arf}$ (Abcam); $p27^{kip1}$ (BD Bioscience); Sox10 (U.S. Biological); Pax3 (kind gift of Dr. G. Grosveld, St. Jude Children's Research Hospital); and Mitf (kind gift of Dr. H. Yamamoto, Tohoku University, Sendai, Japan).

Whole-mount embryo immunostaining. Whole-mount immunostaining was done as previously described (18) with modifications. Briefly, embryos were fixed in 4% paraformaldehyde and irradiated with 500-W microwaves for 30 s, followed by postfixing for 30 min on ice. Samples were incubated overnight at 4°C with primary antibody anti-Dct (Santa Cruz) and again overnight at 4°C with secondary antibody horseradish peroxidase (HRP)–conjugated antigoat IgG (Bethyl Laboratories).

Immunohistochemistry of mouse skin. Dorsal skin samples were fixed in 4% paraformaldehyde and irradiated with 500-W microwaves for 30 s at 4°C. Cryosections mounted on slides were incubated with primary antibody anti-Dct (Santa Cruz) and secondary antibody Alexa 546–conjugated antigoat (Molecular Probes). Samples were counterstained with YO-PRO-1 iodide (Molecular Probes). For quantitation, the numbers of Dct^+ cells in 10 randomly chosen microscopic fields covering an area of 0.138 mm^2 per field were counted per mouse.

Histologic analysis of tumors. Tumor samples were either fixed in 4% paraformaldehyde and embedded in paraffin or embedded in optimum cutting temperature compound and snap frozen. Paraffin-embedded samples were preincubated with 0.3% H_2O_2 in methanol to block endogenous peroxidase activity. Primary and secondary antibodies used to detect the melanoma markers S100 and Melan-A were: rabbit anti-S100 (DAKO) plus biotinylated goat anti-rabbit IgG (DAKO) and anti–Melan-A (DAKO) plus Envision+ detection system-HRP (DAKO). Dct staining was done as described above. For Dopa staining, cryosections were fixed in acetic acid/formaldehyde/ethanol (1:2:17) for 1 min at room temperature followed by incubation in 0.1% DL-Dopa (Sigma) in phosphate buffer (pH 7.4) at 37°C for 4 h. Hematoxylin was used for counterstaining.

Depilation. Anesthetized male mice (>40 d old) in the second telogen phase were shaved and embedded dorsal fur was gently removed with adhesive tape (Kanebo). Depilations were repeated for up to five times at intervals of approximately 4 wk, when all hair follicles of the dorsal skin were in telogen (as judged by their pink skin color). Evaluation of hair graying was done at 3 wk after the last depilation. Administration of ACK2 was done as described (19) with modifications. Briefly, ACK2 (25 mg/kg) was injected into the peritoneal cavity on day 1, 2, or 3 after hair plucking and mouse skin was harvested on day 8.

Hair follicle whole mounts. Whole mounts of mouse hair follicles were prepared and examined as described (20) with modifications. Briefly, mouse dorsal skin harvested at day 8 after hair plucking (mid-anagen) was incubated in 1 mg/mL collagenase IV (Invitrogen) in PBS at 37°C for 1 h. The thick adipose tissue was removed with fine forceps. Samples were fixed and immunostained to detect Dct as described above. Individual hair follicles were isolated from the stained epidermal sheets using a dissecting microscope. Hair follicles were counterstained with 4′,6-diamidino-2-phenylindole (DAPI; Chemicon).

To detect MSCs and melanocytes in the shaft base of a plucked hair, hair follicles were secured on strips of adhesive tape and immunostained first with anti-Dct and Alexa 546–conjugated antigoat IgG, then with anti-CD34 (BD Bioscience), and finally with Alexa 488–conjugated antirat IgG (Molecular Probes). Images were acquired using a Zeiss LSM510 confocal microscope. Each hair follicle was scanned horizontally as a *z*-projection to a total thickness of 30 to 80 μm (includes the bulb and bulge). For quantitation, calculations were based on the average numbers of Dct^+ cells (melanocytes) and $CD34^{high}$ cells (niche of MSCs) in the shaft base of ~10 randomly chosen hair follicles/mouse.

Melanoma induction. To induce tumorigenesis, the backs of 3-wk-old mice were shaved and treated topically with a single 0.5-mg dose of 7,12-dimethylbenz[*a*]anthrcene (DMBA; Sigma) in acetone. Two weeks later, the same area was topically treated with 5 μg of phorbol-12-myristate-13-acetate (TPA; Sigma) in ethanol twice weekly for 24 wk.

Cell size of cultured melanocytes. Cultured melanocytes (2×10^5) were replated in type I collagen–coated 35-mm dishes and cultured for 24 h in melanocyte-defined medium containing 2% fetal bovine serum. Cell area was determined using Image J software. Calculations were based on the average area of 100 randomly chosen melanocytes. Cell size was confirmed by flow cytometry using a Cytomics FC500 (Beckman Coulter) to evaluate forward scatter (FSC).

Pten reintroduction via lentivirus. For a detailed discussion, see Supplementary data.

Results

Generation of mice bearing Pten-deficient melanocytes. We generated a conditional mutant in which Pten expression was governed by the *Dct* (*Trp2*) promoter, which is active in pigment-producing cells and some neuronal cells. In a normal E12.5 embryo, the Dct promoter directs gene expression in the telencephalon, retinal pigment epithelium, melanoblasts, and MSCs (21). We crossed $Pten^{flox/flox}$ mice (17) with *DctCre* transgenic mice (21) to generate mice bearing Pten-deficient melanocytes (Supplementary Fig. S1*A*). Quantitative PCR analysis confirmed that the efficiency of Cre recombination in total cultured primary melanocytes of $DctCrePten^{flox/flox}$ mice was about 70% to 75% (Supplementary Fig. S1*B*). [Quantitation was established in preliminary PCR experiments using mixtures of various ratios of $Pten^{\Delta}$ and $Pten^{flox}$

plasmid DNAs under identical PCR conditions (Supplementary Fig. S1*C*).] Western blotting of cultured primary *DctCrePten*$^{flox/flox}$ melanocytes confirmed that Pten protein was proportionately reduced in these cells (Supplementary Fig. S1*D*), and immunohistochemical analysis showed that 92% to 98% of these melanocytes were Dct^{+} (data not shown).

Neurologic defects cause premature lethality of *DctCrePten*$^{flox/flox}$ mice. *DctCrePten*$^{flox/flox}$ mice were born healthy at the expected Mendelian ratio but ~50% of them died within 2 months of birth due to a neurologic abnormality that resulted in severe immobility. Animals that survived for >2 months had shortened life spans (Fig. 1*A*) and were small compared with control littermates (Fig. 1*B*). Surviving mutants also exhibited immobility and staring (>80%), hyperirritability (~50%), tonic and clonic convulsions (10%), and deep sensory disturbance (10%). On dissection, *DctCrePten*$^{flox/flox}$ brains were substantially larger than those of age-matched controls, especially in the cerebral cortex and hippocampus (Fig. 1*C, top, middle*). Histologically, the cells in these brain structures in *DctCrePten*$^{flox/flox}$ mice had more cytoplasm and larger nuclei (Fig. 1*C, bottom*), similar to *GfapCrePten*$^{flox/flox}$ mice (22). There were no obvious abnormalities in the olfactory bulb, thalamus, or cerebellum (data not shown). Interestingly, no differences between *DctCrePten*$^{flox/flox}$ and control adult mice were observed in hair color (Fig. 1*B*), pigmentation of the skin (data not shown), or pigmentation of the retinal pigment epithelium, iris, or ciliary body of the eye (Fig. 1*D*). Thus, although the loss of Dct-controlled Pten expression profoundly alters brain architecture and results in neurologic symptoms, this mutation has a more subtle effect on pigmented areas of the body.

Increased number of dermal melanocytes in perinatal *DctCrePten*$^{flox/flox}$ mice. Dct is activated in all melanocyte lineage cells starting at E10.5. We quantitated the numbers of Dct^{+} cells in the dermis and epidermis of *DctCrePten*$^{+/+}$ and *DctCrePten*$^{flox/flox}$ mice to compare the numbers of melanocytes and their precursors during embryogenesis. In wild-type (WT) mice, the numbers of epidermal and dermal melanocytes start to increase no later than E16.5. Epidermal melanocyte numbers increase until postnatal days 4 to 5 and then sharply decrease, whereas dermal melanocyte numbers undergo a mild reduction that starts right after birth (23). This pattern held true in our *DctCrePten*$^{+/+}$ mice but the number of Dct^{+} melanocytes in *DctCrePten*$^{flox/flox}$ dermis was increased by up to 2-fold over that in control littermates from E18.5 to postnatal day 5 (Fig. 2*A* and *B*, *bottom*). In contrast, the number of Dct^{+} melanocytes in *DctCrePten*$^{flox/flox}$ epidermis tended to be slightly lower than in control epidermis (Fig. 2*B, top*). By postnatal day 21, there was no difference between control and mutant mice in the number of Dct^{+} melanocytes in the dermis or epidermis (Fig. 2*B*). Thus, Dct-controlled Pten deficiency *in vivo* affects dermal, but not epidermal, morphogenesis.

Resistance of *DctCrePten*$^{flox/flox}$ mice to hair graying due to decreased exhaustion of MSCs. During human aging, cyclic reconstruction of an intact hair follicle pigmentary unit occurs for only the first 10 cycles (i.e., up to ~40 years of age). Thereafter, hair follicle pigmentary potential is spent, leading to hair graying (4). Natural aging in most mouse strains also results in hair graying (4), but only faint graying of the hair and whiskers is seen in aged C57BL/6 mice. In general, mice are naturally more resistant than humans to hair graying because mouse hair follicles can contain hairs that were formed during previous hair cycles. In contrast, human hair follicles possess only a single hair and each follicle sheds its hair during anagen when a new hair grows (24). The multiple hairs in mouse follicles make it difficult to study hair graying in unmanipulated mouse populations. Depilation (hair plucking) during telogen is the foremost artificial means of achieving synchronous anagen, and experimental hair graying in

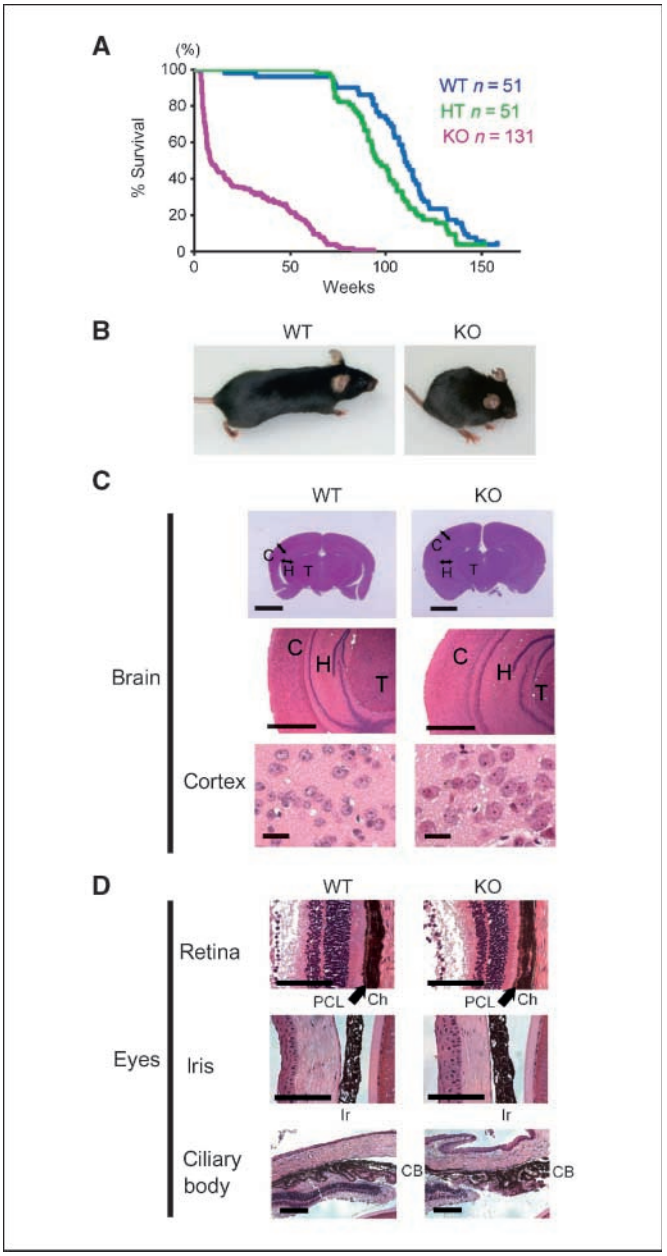

Figure 1. DctCrePten$^{flox/flox}$ mice die prematurely due to neurologic abnormalities. *A,* decreased survival. Kaplan-Meier analyses of the survival of untreated *DctCrePten*$^{+/+}$ (WT), *DctCrePten*$^{flox/+}$ (*HT*), and *DctCrePten*$^{flox/flox}$ (KO) mice. The survival of KO mice was significantly decreased relative to that of WT or *DctCrePten*$^{flox/}$ mice ($P < 0.0001$, log-rank test). *B,* decreased body size but normal hair pigment. Adult WT and KO mice (7 mo old) show a great difference in body size but have indistinguishable coat colors. *C,* brain abnormalities. *Top,* marked macrocephaly in KO mice. *C,* cerebral cortex; *H,* hippocampus; *T,* thalamus. *Bar,* 2 mm. *Middle,* macroencephaly in the cerebral cortex and hippocampus of KO mice. *Bar,* 1 mm. *Bottom,* individual neurons in the granular layer of the cerebral cortex, as well as the nuclei of these cells, are increased in size in the mutant. *Bar,* 50 μm. *D,* normal pigment in the eyes. The retinal pigment epithelium (*top*), iris pigment epithelium (*middle*), and ciliary body (*bottom*) are all tissues in which Dct is expressed. No obvious histologic abnormalities were seen in KO mice. *PCL,* pigment cell layer; *Ch,* choriodea; *Ir,* iris; *CB,* ciliary body. *Bar,* 100 μm.

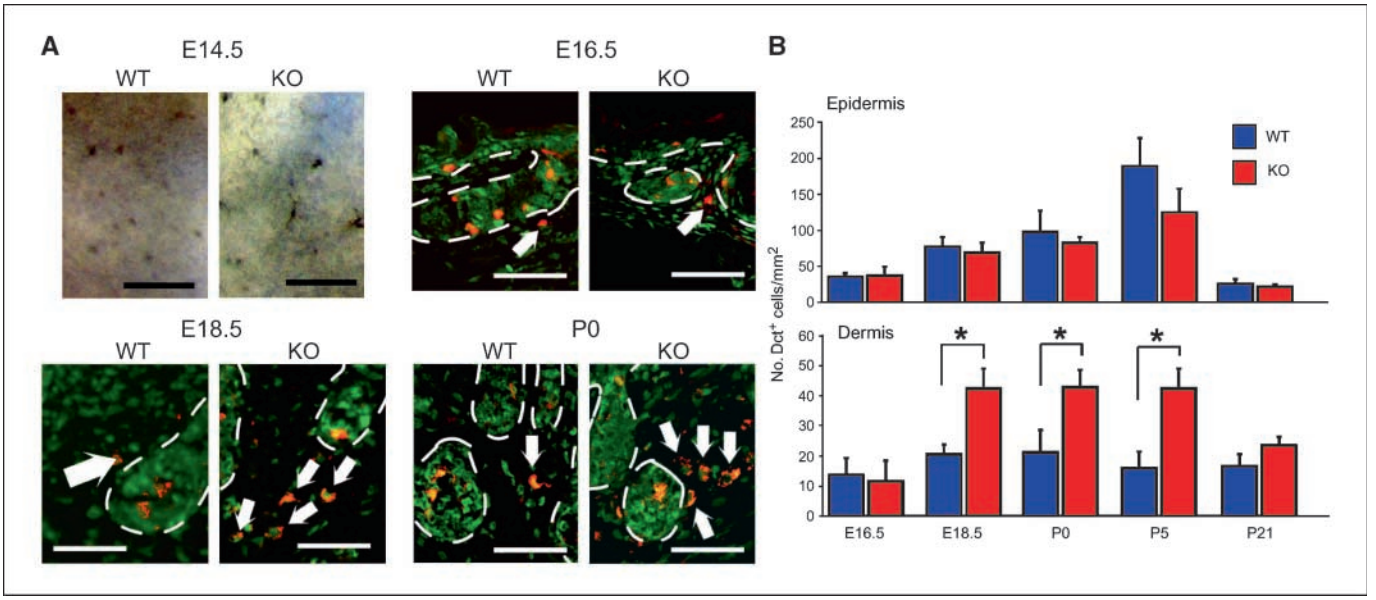

Figure 2. Increased number of melanocytes in the dermis of perinatal DctCrePten$^{flox/flox}$ mice. *A,* immunostaining. Whole-mount embryo immunostaining (*top left*) and immunofluorescent staining (*top right* and *bottom*) were used to analyze skin sections of *DctCrePten*$^{+/+}$ (WT) and *DctCrePten*$^{flox/flox}$(KO) mice sacrificed on the indicated day. *Top left,* detection of melanocytes with anti-Dct antibody. *Top right* and *bottom, red,* anti-Dct antibody detecting melanocytes; *green,* YO-PRO-1 staining to visualize nuclei; *dotted lines,* dermal-epidermal junctions; *white arrows,* dermal melanocytes. *Bar,* 100 μm. *B,* quantitation. The numbers of melanocytes/mm^2 in the epidermis and dermis of WT and KO mice were determined on the indicated days. *Columns,* mean of three mice per group; *bars,* SE. Representative of 10 trials. *, $P < 0.05$, Student's *t* test.

C57BL/6 mice can be induced by repeated depilation during telogen (25).

To examine hair graying in the absence of Pten, we subjected *DctCrePten*$^{+/+}$ and *DctCrePten*$^{flox/flox}$ mice to repeated depilations. Whereas *DctCrePten*$^{+/+}$ mice gradually lost pigmentation and became gray, *DctCrePten*$^{flox/flox}$ mice maintained their black coats (Fig. 3*A, top*). To quantify hair graying, we devised a hair graying score (Fig. 3*A, bottom*). Analysis of the percentage of control and mutant mice with each hair graying score revealed that *DctCrePten*$^{flox/flox}$ mice were resistant to hair graying induced by repeated depilation (Fig. 3*B*; $P < 0.01$).

Defective maintenance of MSCs is known to lead to hair graying (4). Because MSCs are a rare population, the removal of differentiated melanocytes from a hair follicle makes the analysis of MSCs in this follicle easier. ACK2 is an antagonistic monoclonal antibody directed against c-Kit (18). I.p. injection of ACK2 into WT mice after the first hair plucking effectively depletes melanocytes and amplifies melanoblasts in the bulb and bulge of the hair follicle. The MSCs, which are c-Kit independent, are left intact and can restore pigment to the hair in a later hair cycle (2). We confirmed these findings in our *DctCrePten*$^{+/+}$ mice (Supplementary Fig. S2*A*) and showed by Dct staining of whole mounts of hair follicles that MSCs were intact in the bulge (Supplementary Fig. S2*B*).

To determine the localization and number of Dct$^+$ MSCs in *DctCrePten*$^{flox/flox}$ hair follicles, we administered 25 mg/kg ACK2 to *DctCrePten*$^{+/+}$ and *DctCrePten*$^{flox/flox}$ mice and examined MSCs in hair follicles at mid-anagen (8 days after depilation). There were no differences between control and mutant mice in the numbers of Dct$^+$ melanoblasts and Dct$^+$/c-Kit–independent MSCs in the bulge (Fig. 4*A* and *B*) or of Dct$^+$ melanocytes in the bulb (data not shown). However, after four depilations, the MSCs in the bulge in control follicles were clearly exhausted, as evidenced by their dramatically decreased numbers (Fig. 4*B*). In contrast, MSCs in *DctCrePten*$^{flox/flox}$ hair follicle bulges resisted exhaustion.

When a hair is removed (even at telogen), there is inevitably some mechanical loss of hair follicle keratinocytes, melanocytes (including MSCs; ref. 26), and/or bulge cells (the MSC niche; ref. 27). To evaluate whether the reduced depilation-induced hair graying in *DctCrePten*$^{flox/flox}$ mice was due to decreased mechanical loss of melanocytes/MSCs and/or the MSC niche, we immunostained the shaft base of each plucked hair with antibodies recognizing Dct or CD34 (a marker for bulge cells 28). No differences were observed between control and mutant mice in the number of Dct$^+$ cells (Fig. 4*C, left*) or CD34^{high} cells (Fig. 4*C, right*) in the shaft base of plucked hairs. Thus, we believe that the lack of depilation-induced hair graying in *DctCrePten*$^{flox/flox}$ mice is not simply due to reduced mechanical loss of MSCs but rather to Pten inactivation that prevents MSC exhaustion.

Increased susceptibility of *DctCrePten*$^{flox/flox}$ mice to carcinogen-induced melanomas. Although 9% of *DctCrePten*$^{flox/flox}$ mice developed spontaneous neurofibromas (Supplementary Fig. S3), no mutants developed spontaneous melanomas. To determine whether *DctCrePten*$^{flox/flox}$ mice were predisposed to melanoma induction, we used the classic DMBA plus TPA two-step carcinogenic protocol that induces the rapid development of skin papillomas and small nevi. By 15 wk after DMBA treatment, 78% of both *DctCrePten*$^{+/+}$ and *DctCrePten*$^{flox/flox}$ mice had developed papillomas and 94% had developed small nevi (<3 mm; Fig. 5*A*). However, large nevi [>3 mm; Fig. 5*A*(*b*) and *C*(*a*)] occurred more frequently in *DctCrePten*$^{flox/flox}$ mice than in controls (53.1% versus 8.5%; $P < 0.0001$), as did invasive spindle cell melanomas [25.9% versus 2.1%; $P < 0.0001$; Fig. 5*A*(*c*) and *C*(*b*)-(*g*)].

We confirmed our histologic identification of melanomas in *DctCrePten*$^{flox/flox}$ mice by immunostaining to detect Dct [Fig. 5*C*(*c*)], the melanocyte differentiation antigen Melan-A [Fig. 5*C*(*d*)], and the Dopa reaction [which is positive in tyrosinase-containing melanocytes; Fig. 5*C*(*e*)]. Melanomas in the mutants were also positive for the neuroectodermal marker S100

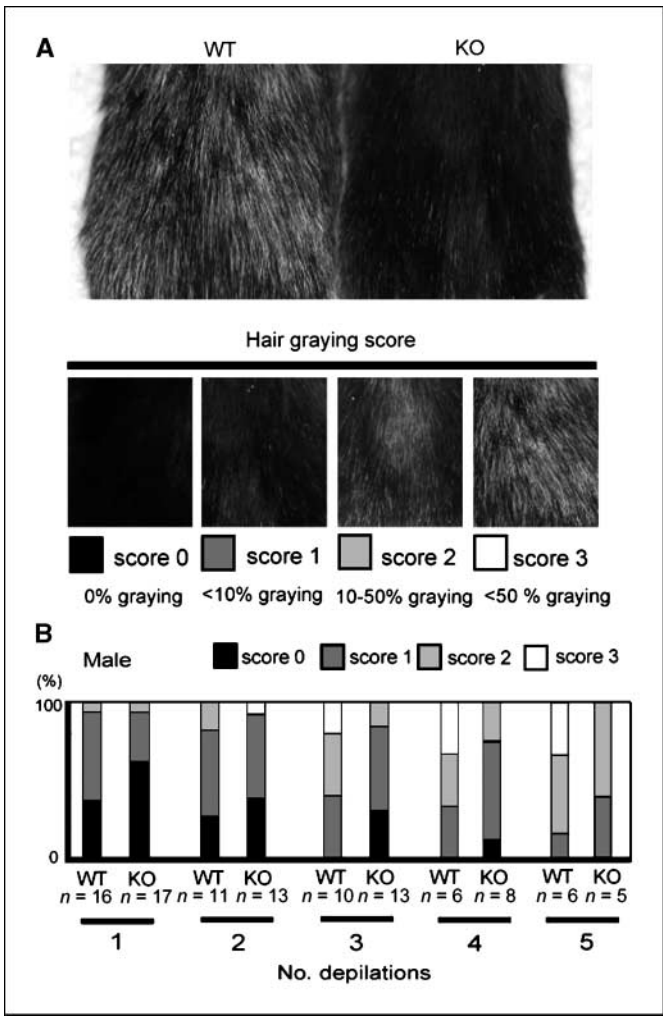

Figure 3. Resistance to hair graying in DctCrePten$^{flox/flox}$ mice. *A,* images of hair graying. *Top,* representative appearance of a *DctCrePten*$^{+/+}$ mouse (WT; hair graying score 3) and a *DctCrePten*$^{flox/flox}$ mouse (KO; hair graying score 1) after five depilations. *Bottom,* the hair graying score was defined as indicated. *B,* prevalence of hair graying in male mice. Results shown are the percentages of WT and KO mice examined that showed the indicated hair graying scores after one to five depilations. KO mice showed significant resistance to hair graying after repeated hair plucking ($P < 0.01$, nonparametric Mann-Whitney *U* test). Representative of four trials.

[Fig. 5*C*(*f*)]. Furthermore, 20% (2 of 10) of melanoma-bearing mice showed lung metastasis [Fig. 5*C*(*g*)]. Thus, *DctCrePten*$^{flox/flox}$ mice show increased susceptibility to carcinogen-induced melanomagenesis.

Pten-deficient melanocytes show enlarged cell size and altered signaling molecule expression. We next set out to elucidate the signaling molecules responsible for both the resistance of Pten-deficient MSCs to exhaustion and the increased tumor susceptibility of *DctCrePten*$^{flox/flox}$ mice. Primary melanocytes were isolated from the dorsal skin of neonatal control and mutant mice and cultured for 14 days. Cultured *DctCrePten*$^{flox/flox}$ melanocytes showed wide variation in cell size and shape but were larger than cultured WT melanocytes (Fig. 6*A*). We confirmed the increased cell size of the mutant melanocytes by flow cytometric evaluation of FSC. Moreover, we showed that this enlargement could be rescued by lentivirus-mediated reintroduction of Pten [mean FSC ± SE values were 250 ± 1.28 (WT) versus 257 ± 0.474 (KO) versus 247 ± 2.00 (KO + Pten); $n = 3$ mice per group].

A spectrum of molecules involved in melanocyte apoptosis, differentiation, or melanin synthesis are important for hair graying in mice, including Bcl-2, Pax3, Sox10, Mitf, c-Kit, Notch, tyrosinase, Trp1, and Dct (5, 6, 29). We used Western blotting to examine these molecules in control and mutant cultured primary melanocytes.

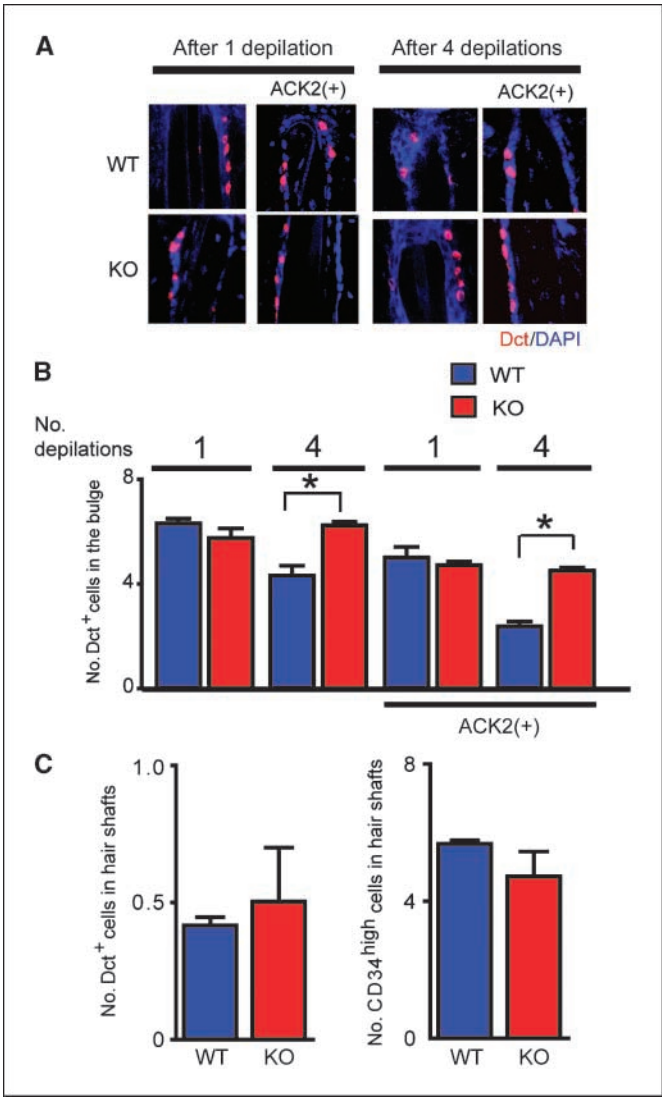

Figure 4. Resistance of DctCrePten$^{flox/flox}$ MSCs to exhaustion induced by repeated depilation. MSCs were examined in hair follicle bulges of *DctCrePten*$^{+/+}$ (WT) and *DctCrePten*$^{flox/flox}$ (KO) mice that were subjected to one or four depilations. *A,* MSC visualization. Representative whole mounts of hair follicles were stained with DAPI (*blue*) to detect nuclei and anti-Dct (*red*) to detect melanoblasts and MSCs in the bulge. ACK2 antibody was used to deplete c-Kit^{+} melanocytes in the bulb and bulge and thus enhance visualization of MSCs. *B,* intact MSC numbers after depilation. MSCs in the bulges in *A* were quantitated by counting ACK2-resistant Dct^{+} cells. *Columns,* mean of five mice per group; *bars,* SE. Representative of 10 trials. *, $P < 0.05$, Student's *t* test. *C,* no decrease in mechanical loss of melanocytes/MSCs and bulge cells. Plucked hairs from WT and KO mice were secured on adhesive tape and the shaft base of hairs was double immunostained with anti-Dct and anti-CD34 antibodies to detect melanocytes/MSCs and bulge cells (niche of MSCs), respectively. Ten plucked hairs per mouse were randomly chosen and analyzed. *Columns,* mean numbers of Dct^{+} and CD34^{high} cells per plucked hair from three WT and three KO mice; *bars,* SE. Representative of three trials. No differences between WT and KO mice were observed.

Bcl-2 expression was markedly up-regulated in Pten-deficient melanocytes (Fig. 6*B*). However, there were no differences between the genotypes in eight other signaling molecules. Bcl-2 deficiency triggers apoptosis selectively in MSCs within the bulge (4), leading to MSC exhaustion. Thus, the resistance to exhaustion of *DctCrePten*$^{flox/flox}$ MSCs may be due to enhanced Bcl-2 expression.

Several downstream effectors of the PTEN/PI3K pathway are reportedly involved in melanomagenesis, including Akt (4) and Erks (15). We used Western blotting to examine these molecules in cultured primary melanocytes from neonatal *DctCrePten*$^{+/+}$, *DctCrePten*$^{flox/+}$, and *DctCrePten*$^{flox/flox}$ mice and in melanoma cells from DMBA/TPA–treated *DctCrePten*$^{flox/flox}$ mice. Compared with *DctCrePten*$^{+/+}$ and *DctCrePten*$^{flox/+}$ controls, *DctCrePten*$^{flox/flox}$ melanocytes showed significantly increased phosphorylation of Akt and Erks but decreased p27^{kip1} expression (Fig. 6*C*). The mutant cells also showed increased expression of p19^{Arf}, p21$^{cip/waf1}$, and p53 (Fig. 6*C*). Although the elevated Akt activation in the Pten-deficient cells was completely abolished by treatment with the PI3K inhibitor wortmannin (as expected), the increased Erk activation was not (Fig. 6*D*). Compared with cultured *DctCrePten*$^{flox/flox}$ melanocytes, melanoma cells from DMBA/TPA–treated *DctCrePten*$^{flox/flox}$ mice showed equivalent Akt activation but heightened Erk activation, decreased p27^{kip1} expression, and a greater increase in p16^{Ink4a} and p19^{Arf} expression (Fig. 6*C*). Thus, melanoma onset in carcinogen-treated *DctCrePten*$^{flox/flox}$ mice may be due to alterations in PI3K-dependent Akt activation and PI3K-independent Erk activation and the effects of these alterations on p27^{kip1} and Bcl-2.

Discussion

PTEN protein expression is decreased or lost in many sporadic melanomas (12). In addition, melanomas are sometimes found in Cowden disease patients who bear a heterozygous germ-line mutation of PTEN. The characteristic clinical features of Cowden disease include benign skin abnormalities such as trichilemmomas, papules, papillomatosis, hyperkeratosis, and a variety of pigmentary changes such as lentigines, café-au-lait spots, and acromelanosis

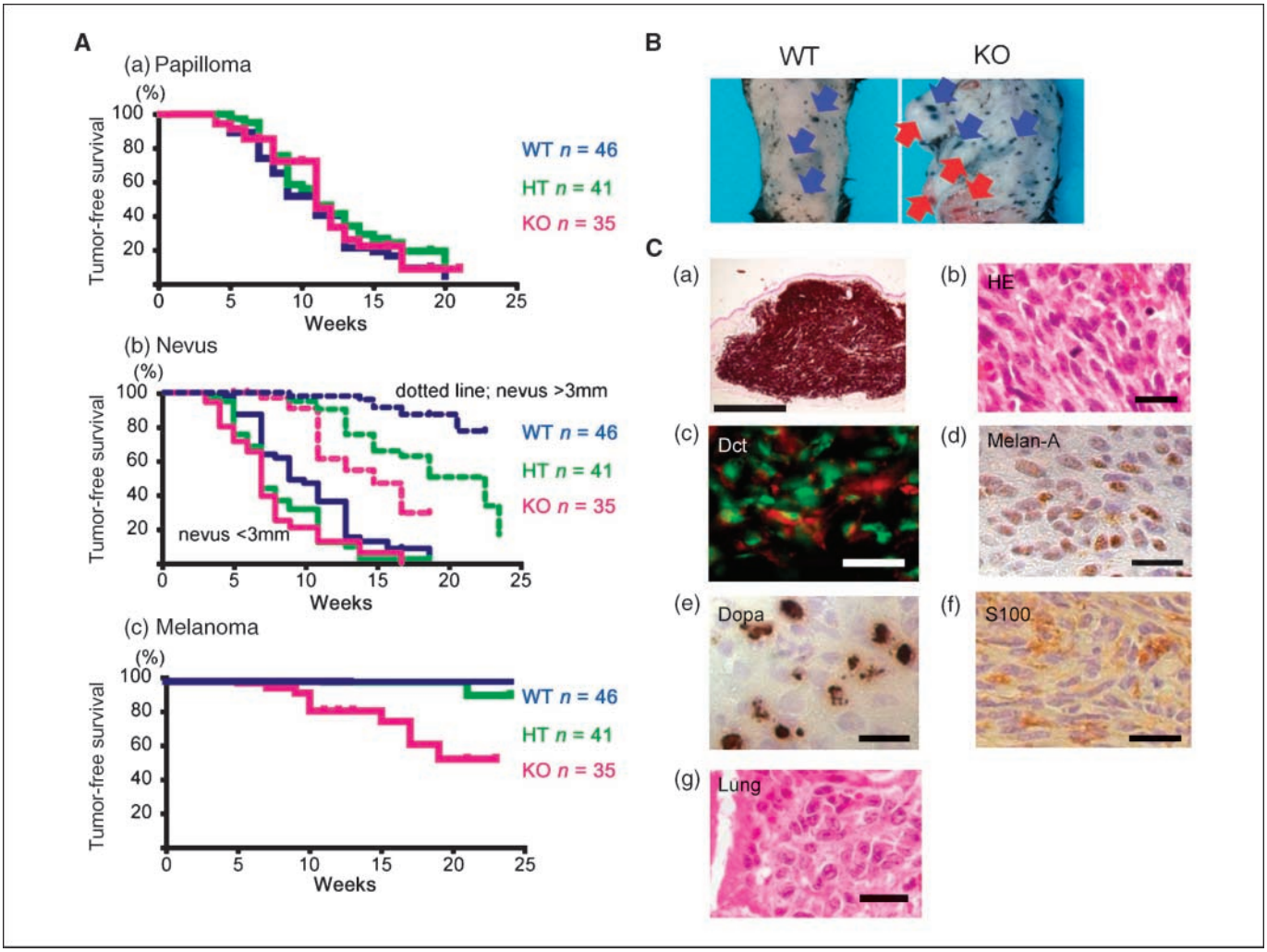

Figure 5. Carcinogen-induced formation of large nevi and spindle cell melanomas in DctCrePten$^{flox/flox}$ mice. *A,* tumor incidence. *DctCrePten*$^{+/+}$ (WT), *DctCrePten*$^{flox/+}$ (*HT*), and *DctCrePten*$^{flox/flox}$ (KO) mice were treated with DMBA/TPA and monitored for 24 wk for skin tumor development. Kaplan-Meier survival analyses show the percentages of these mice that developed papillomas (*a*), nevi (*b*; *solid line,* <3 mm; *dotted line,* >3 mm), or melanomas (*c*). *B,* representative macroscopic nevi (*blue arrows*) and melanomas (*red arrows*) that developed in WT and KO mice at 20 wk after DMBA/TPA treatment. *C*, histology. *a,* H&E-stained section of a large nevus in a KO mouse. *Bar,* 1 mm. *b,* H&E-stained section of a low-grade spindle cell melanoma in a KO mouse. *c,* melanoma stained with anti-Dct (*red*) and counterstained with YO-PRO-1 (*green*). *d,* melanoma immunostained to detect Melan-A. *e,* melanoma showing positivity for the Dopa reaction. *f,* melanoma immunostained to detect S100. *g,* H&E-stained lung of a KO mouse showing metastatic melanoma cells. *Bar,* 20 μm (*b–g*).

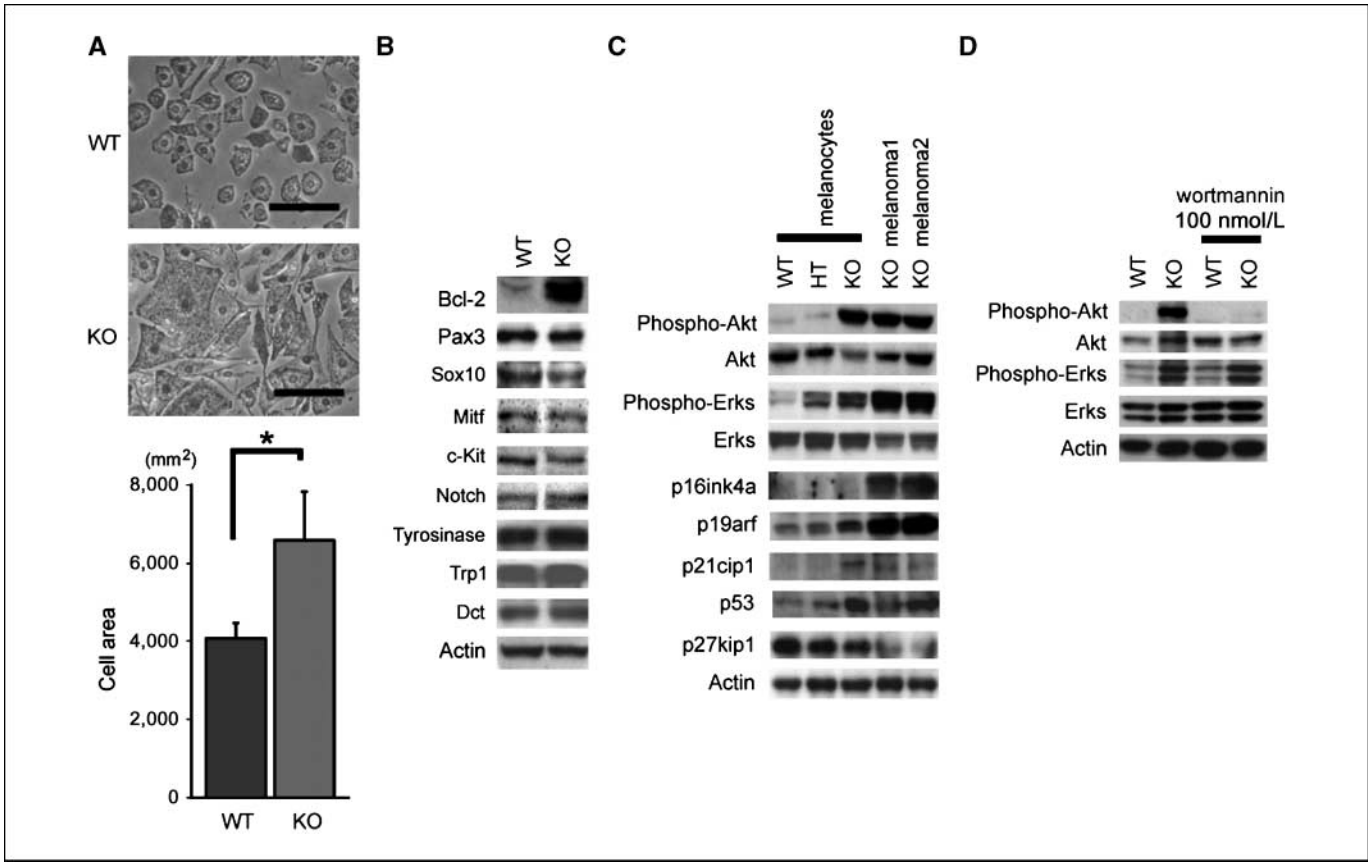

Figure 6. DctCrePten$^{flox/flox}$ cultured melanocytes are increased in size and show altered signaling. *A,* increased cell size. *Top,* representative morphology. *DctCrePten$^{flox/flox}$* (KO) cultured melanocytes are significantly larger than *DctCrePten$^{+/+}$* (WT) cultured melanocytes. *Bar,* 100 μm. *Bottom,* quantitation. *Columns,* mean cell area (n = 100 cells per genotype); *bars,* SE. *, $P < 0.05$, Student's t test. *B,* altered melanocyte protein expression. The expression levels of the indicated proteins important for melanocyte apoptosis, differentiation, or melanin synthesis were examined by immunoblotting of primary melanocyte cultures from WT and KO mice. *C,* altered melanoma-related protein expression. The expression or activation of the indicated molecules important for melanomagenesis was examined in the cultures in *A* as well as in two melanomas from KO mice. *D,* activation of Erk1/2 is PI3K independent. In KO melanocytes, addition of the PI3K inhibitor wortmannin completely abolished Akt phosphorylation but did not affect Erk1/2 phosphorylation. *B* to *D,* total Akt, total Erks, and actin were evaluated as controls. Representative of three trials.

(30). However, little is known about the function of PTEN in melanocytes *in vivo*. In this study, we generated mice with a conditional deficiency of Pten in melanocytes and examined hair graying and melanomagenesis in these mutants.

Resistance to hair graying. The melanocyte phenotype of *DctCrePten$^{flox/flox}$* mice was relatively mild in that only a small increase in dermal melanocyte numbers was observed at the perinatal stage. However, adult *DctCrePten$^{flox/flox}$* mice were resistant to hair graying induced by repeated depilation.

PTEN regulates cell cycling, apoptosis, differentiation, and migration by controlling the PI3K-Akt and Ras-Erk signaling pathways. In addition, Pten influences tissue-specific stem cell numbers because Pten deletion leads to stem/progenitor cell expansion in the prostate gland (31), central nervous system (32), and bronchioalveolar epithelium (33) and also promotes leukemia stem cell generation (34). Consistent with these observations, the PI3K-Akt pathway mediates the self-renewal of mouse spermatogonial stem cells (35), and mitogen-activated protein kinase (MAPK) is required for the maintenance of human epidermal stem cells and neural stem cells (36). The numbers of tissue-specific stem cells are also controlled by cyclin-dependent kinase (CDK) inhibitors because loss of p27^{kip1} or mitotic arrest deficiency 1, which are negative cell cycle regulators, increases the hematopoietic stem cell pool and causes these cells to more rapidly enter the cell cycle (37). Thus, multiple signaling mechanisms involving Akt, MAPK, and/or CDK inhibitors seem to act downstream of Pten and affect MSC maintenance *in vivo*.

Hair graying is directly governed by genes that are involved in MSC maintenance, melanocyte differentiation, or melanin granule synthesis. We screened for the expression of nine such genes and found a marked increase in Bcl-2 expression in Pten-deficient melanocytes. Transgenic Bcl-2 expression in hematopoietic stem cells inhibits apoptosis, resulting in increased hematopoietic stem cell numbers (38). Bcl-2$^{-/-}$ mice prematurely turn gray due to the disappearance of melanocytes and MSCs, suggesting that Bcl-2 protects MSCs from succumbing to apoptosis during entry into quiescence (4, 5). In many cell types, Bcl-2 expression is up-regulated by Akt or Erk activation (39, 40). Thus, the enhanced Bcl-2 expression observed in Pten-deficient melanocytes may be due to the increased activation of Akt and Erks that occurs in the absence of Pten. This increased Bcl-2 may protect MSCs from exhaustion and cause *DctCrePten$^{flox/flox}$* mice to resist hair graying.

Repeated hair plucking at telogen synchronizes MSCs in anagen and induces their premature exhaustion by inducing apoptosis during entry into catagen (3). In addition, repeated depilation may cause some physical loss of nonapoptotic (live) melanocytes/

MSCs and/or their niche (niche wounding) in the shaft base of a plucked hair even when depilation occurs at telogen (2). However, the resistance to hair graying in depilated *DctCrePten$^{flox/flox}$* mice was not simply due to a relative decrease in such mechanical loss because no differences between *DctCrePten$^{+/+}$* and *DctCrePten$^{flox/flox}$* mice were observed in the numbers of Dct^{+} and CD34^{high} cells found in the shaft base of plucked hairs. In contrast to depilation, physiologic hair shedding does not cause MSC niche wounding, and there are dead cells in the shaft base as a consequence of apoptosis during exogen (41). Thus, although hair shedding and depilation differ with respect to timing of melanocyte apoptosis and occurrence of MSC niche wounding, apoptosis probably remains very important for hair graying caused by either process. Our study showed that the numbers of MSCs and melanoblasts in hair follicle bulges did not increase in *DctCrePten$^{flox/flox}$* mice without repeated depilation. Thus, resistance to apoptosis, rather than enhanced cell cycle entry, seems to be the more likely explanation for the resistance of Pten-deficient MSCs to exhaustion.

Susceptibility to carcinogen-induced melanomagenesis. *DctCrePten$^{flox/flox}$* mice did not develop spontaneous melanomas but were abnormally susceptible to the chemical induction of spindle cell melanomas. In humans, spindle cell melanomas are aggressive and immature tumors of neuroectodermal origin (7). We speculate that the exhaustion-resistant MSCs of *DctCrePten$^{flox/flox}$* mice run an increased risk of acquiring multiple oncogenic mutations and becoming cancerous, perhaps eventually generating spindle cell melanomas. These Pten-deficient MSCs may even serve as melanoma cancer stem cells, parallel to the stem cell involvement noted in hematopoietic malignancies (34). Nevertheless, our findings show that Pten deficiency must be combined with additional oncogenic mutation(s) to trigger melanomagenesis.

The Ras-Erk (MAPK), p16^{Ink4a}-Rb, p19^{Arf}-p53, and PI3K-Akt3 pathways are all linked to melanoma formation (7). However, the alteration of a single molecule in any one of these pathways rarely induces melanomagenesis *in vivo*. To date, double mutations of p16$^{Ink4a-/-}$/p19$^{Arf+/-}$ (42) or p53$^{-/-}$/H-Ras^{V12G} (43) or triple mutations of H-Ras^{V12G}/p16$^{Ink4a-/-}$/p19$^{Arf-/-}$ (44), N-Ras^{Q61K}/p16$^{Ink4a-/-}$/p19$^{Arf-/-}$ (45), or Pten$^{+/-}$/p16$^{Ink4a-/-}$/p19$^{Arf-/-}$ (46) have been necessary to reliably induce melanomas in mice. This structure likely explains why no spontaneous melanomas occurred in our *DctCrePten$^{flox/flox}$* mice despite the Pten deficiency in their melanocytes.

Melanocytes from *DctCrePten$^{flox/flox}$* mice showed Akt and Erk activation as well as increased Bcl-2 and reduced p27^{kip1} expression. These alterations likely contributed to the increased dermal melanocytes in perinatal *DctCrePten$^{flox/flox}$* mice, the resistance of their MSCs to exhaustion, and the onset of carcinogen-induced melanomas. Pten-deficient cells usually show activation of Akt and Erks (17), and it is therefore intriguing that the Erk activation in Pten-deficient melanocytes was PI3K independent. It may be that the protein phosphatase activity of Pten, rather than its lipid phosphatase activity, is important for Erk activation in the mutant melanocytes. Such a scenario would parallel the induction of keratinocyte-derived tumors in mice, which requires Akt signaling in addition to son-of-sevenless/Ras/Erk signaling (47). Erks can also act in synergy with the PI3K pathway to stimulate CycD1 transcription in NIH 3T3 cells (48). Thus, the onset of tumors in *DctCrePten$^{flox/flox}$* mice may be caused by synergistic activation of Akt and Erks. The Erks were more highly activated than Akt in carcinogen-induced tumors of *DctCrePten$^{flox/flox}$* mice, suggesting that an oncogenic signal resulting in strong Erk activation may be required for melanomagenesis.

In addition to Akt and Erk alterations, Pten-deficient melanocytes showed increased expression of p53, p19^{Arf}, and p21$^{cip/waf1}$ and decreased expression of p27^{kip1}. In Pten-deficient melanomas, p16^{INK4a} and p19^{Arf} were further increased and p27^{kip1} was further decreased. Overexpression of Ras^{V12}, Raf1, or BRAF^{E600} by human fibroblasts induces p16^{INK4a} and triggers oncogene-induced cellular senescence, and sustained BRAF^{V600E} expression does the same in human melanocytes (49). Thus, the increased p16^{INK4a} in our Pten-deficient melanocytes may be due to activation of the Erk pathway. The reason why elements of the p19^{ARF}/p53/p21 pathway were elevated in our mutant melanocytes is unknown. However, increased expression of any of these molecules can induce senescence, an occurrence that could have blocked spontaneous melanomagenesis in *DctCrePten$^{flox/flox}$* mice. Indeed, p53-dependent senescence is crucial for the suppression of tumorigenesis in Pten-deficient prostatic cells (50).

Our study is the first functional analysis of Pten in murine melanocytes *in vivo*, and our *DctCrePten$^{flox/flox}$* mouse strain is the first animal model reported to resist hair graying. We have shown that intact Pten-regulated pathways in melanocytes are required for normal hair graying and MSC homeostasis, as well as for the prevention of melanomagenesis. In humans, aging is associated with both hair graying and an accumulated exposure to UV and chemical agents that can increase melanoma risk. Our results suggest that PTEN or its downstream molecules may be attractive cosmetic or therapeutic targets for combating hair graying or melanoma formation. Furthermore, our *DctCrePten$^{flox/flox}$* mice provide a powerful model for investigating the mechanisms underlying these phenomena.

Disclosure of Potential Conflicts of Interest

No potential conflicts of interest were disclosed.

Acknowledgments

Received 3/10/2008; revised 5/7/2008; accepted 5/14/2008.

Grant support: Ministry of Education, Science, Sports, and Culture, Japan (A. Suzuki); Cosmetology Research Foundation (A. Suzuki); and SHISEIDO Grants for Science Research (T. Inoue-Narita).

The costs of publication of this article were defrayed in part by the payment of page charges. This article must therefore be hereby marked *advertisement* in accordance with 18 U.S.C. Section 1734 solely to indicate this fact.

We thank Drs. Junko Sasaki, Yasuo Horie, Shunsuke Takasuga, Miyuki Natsui, and Nao Suzuki (all of Akita University) and Dr. Taiji Yoshida (Research Institute for Brain and Blood Vessels, Akita, Japan) for helpful discussions and technical support; Drs. Kazuhisa Takeda and Hiroaki Yamamoto (both of Tohoku University, Sendai, Japan) for providing anti-Mitf antibody; and Dr. Gerard Grosveld (St. Jude Children's Research Hospital, Memphis, TN) for providing anti-Pax3 antibody.

References

1. Cotsarelis G, Sun TT, Lavker RM. Label-retaining cells reside in the bulge area of pilosebaceous unit: implications for follicular stem cells, hair cycle, and skin carcinogenesis. Cell 1990;61:1329–37.
2. Nishimura EK, Jordan SA, Oshima H, et al. Dominant role of the niche in melanocyte stem-cell fate determination. Nature 2002;416:854–60.
3. Sharov A, Tobin DJ, Sharova TY, Atoyan R, Botchkarev VA. Changes in different melanocyte populations during hair follicle involution (catagen). J Invest Dermatol 2005;125:1259–67.
4. Nishimura EK, Granter SR, Fisher DE. Mechanisms of hair graying: incomplete melanocyte stem cell maintenance in the niche. Science 2005;307:720–4.
5. Veis DJ, Sorenson CM, Shutter JR, Korsmeyer SJ. Bcl-2-deficient mice demonstrate fulminant lymphoid apoptosis, polycystic kidneys, and hypopigmented hair. Cell 1993;75:229–40.

6. Bennett DC, Lamoreux ML. The color loci of mice—a genetic century. Pigment Cell Res 2003;16:333–44.
7. Chin L, Garraway LA, Fisher DE. Malignant melanoma: genetics and therapeutics in the genomic era. Genes Dev 2006;20:2149–82.
8. Li J, Yen C, Liaw D, et al. PTEN, a putative protein tyrosine phosphatase gene mutated in human brain, breast, and prostate cancer. Science 1997;275:1943–7.
9. Maehama T, Dixon JE. The tumor suppressor, PTEN/MMAC1, dephosphorylates the lipid second messenger, phosphatidylinositol 3,4,5-trisphosphate. J Biol Chem 1998;273:13375–8.
10. Gu J, Tamura M, Pankov R, et al. Shc and FAK differentially regulate cell motility and directionality modulated by PTEN. J Cell Biol 1999;146:389–403.
11. Reifenberger J, Wolter M, Bostrom J, et al. Allelic losses on chromosome arm 10q and mutation of the PTEN (MMAC1) tumour suppressor gene in primary and metastatic malignant melanomas. Virchows Arch 2000;436:487–93.
12. Whiteman DC, Zhou XP, Cummings MC, Pavey S, Hayward NK, Eng C. Nuclear PTEN expression and clinicopathologic features in a population-based series of primary cutaneous melanoma. Int J Cancer 2002;99:63–7.
13. Hwang PH, Yi HK, Kim DS, Nam SY, Kim JS, Lee DY. Suppression of tumorigenicity and metastasis in B16F10 cells by PTEN/MMAC1/TEP1 gene. Cancer Lett 2001;172:83–91.
14. Stahl JM, Sharma A, Cheung M, et al. Deregulated Akt3 activity promotes development of malignant melanoma. Cancer Res 2004;64:7002–10.
15. Stahl JM, Cheung M, Sharma A, Trivedi NR, Shanmugam S, Robertson GP. Loss of PTEN promotes tumor development in malignant melanoma. Cancer Res 2003;63:2881–90.
16. Hirobe T. Endothelins are involved in regulating the proliferation and differentiation of mouse epidermal melanocytes in serum-free primary culture. J Investig Dermatol Symp Proc 2001;6:25–31.
17. Suzuki A, Yamaguchi MT, Ohteki T, et al. T cell-specific loss of Pten leads to defects in central and peripheral tolerance. Immunity 2001;14:523–34.
18. Yoshida H, Kunisada T, Kusakabe M, Nishikawa S, Nishikawa SI. Distinct stages of melanocyte differentiation revealed by analysis of nonuniform pigmentation patterns. Development 1996;122:1207–14.
19. Botchkareva NV, Khlgatian M, Longley BJ, Botchkarev VA, Gilchrest BA. SCF/c-kit signaling is required for cyclic regeneration of the hair pigmentation unit. FASEB J 2001;15:645–58.
20. Osawa M, Egawa G, Mak SS, et al. Molecular characterization of melanocyte stem cells in their niche. Development 2005;132:5589–99.
21. Guyonneau L, Rossier A, Richard C, Hummler E, Beermann F. Expression of Cre recombinase in pigment cells. Pigment Cell Res 2002;15:305–9.
22. Backman SA, Stambolic V, Suzuki A, et al. Deletion of Pten in mouse brain causes seizures, ataxia and defects in soma size resembling Lhermitte-Duclos disease. Nat Genet 2001;29:396–403.
23. Kunisada T, Yamazaki H, Hirobe T, et al. Keratinocyte expression of transgenic hepatocyte growth factor affects melanocyte development, leading to dermal melanocytosis. Mech Dev 2000;94:67–78.
24. Dry F. The coat of the mouse (*Mus musculus*). J Genet 1926;16:287–340.
25. Hamilton E, Potten CS. The effect of repeated plucking on mouse skin cell kinetics. J Invest Dermatol 1974;62:560–2.
26. Ibrahim L, Wright EA. The long term effect of repeated pluckings on the function of the mouse vibrissal follicles. Br J Dermatol 1978;99:371–6.
27. Ito M, Kizawa K, Toyoda M, Morohashi M. Label-retaining cells in the bulge region are directed to cell death after plucking, followed by healing from the surviving hair germ. J Invest Dermatol 2002;119:1310–6.
28. Blanpain C, Lowry WE, Geoghegan A, Polak L, Fuchs E. Self-renewal, multipotency, and the existence of two cell populations within an epithelial stem cell niche. Cell 2004;118:635–48.
29. Moriyama M, Osawa M, Mak SS, et al. Notch signaling via Hes1 transcription factor maintains survival of melanoblasts and melanocyte stem cells. J Cell Biol 2006;173:333–9.
30. Hildenbrand C, Burgdorf WH, Lautenschlager S. Cowden syndrome—diagnostic skin signs. Dermatology 2001;202:362–6.
31. Wang S, Garcia AJ, Wu M, Lawson DA, Witte ON, Wu H. Pten deletion leads to the expansion of a prostatic stem/progenitor cell subpopulation and tumor initiation. Proc Natl Acad Sci U S A 2006;103:1480–5.
32. Groszer M, Erickson R, Scripture-Adams DD, et al. Negative regulation of neural stem/progenitor cell proliferation by the Pten tumor suppressor gene *in vivo*. Science 2001;294:2186–9.
33. Yanagi S, Kishimoto H, Kawahara K, et al. Pten controls lung morphogenesis, bronchioalveolar stem cells, and onset of lung adenocarcinomas in mice. J Clin Invest 2007;117:2929–40.
34. Yilmaz OH, Valdez R, Theisen BK, et al. Pten dependence distinguishes haematopoietic stem cells from leukaemia-initiating cells. Nature 2006;441:475–82.
35. Lee J, Kanatsu-Shinohara M, Inoue K, et al. Akt mediates self-renewal division of mouse spermatogonial stem cells. Development 2007;134:1853–9.
36. Zhu AJ, Haase I, Watt FM. Signaling via β1 integrins and mitogen-activated protein kinase determines human epidermal stem cell fate *in vitro*. Proc Natl Acad Sci U S A 1999;96:6728–33.
37. Walkley CR, Fero ML, Chien WM, Purton LE, McArthur GA. Negative cell-cycle regulators cooperatively control self-renewal and differentiation of haematopoietic stem cells. Nat Cell Biol 2005;7:172–8.
38. Domen J, Gandy KL, Weissman IL. Systemic overexpression of BCL-2 in the hematopoietic system protects transgenic mice from the consequences of lethal irradiation. Blood 1998;91:2272–82.
39. Pugazhenthi S, Nesterova A, Sable C, et al. Akt/protein kinase B up-regulates Bcl-2 expression through cAMP-response element-binding protein. J Biol Chem 2000;275:10761–6.
40. Boucher MJ, Morisset J, Vachon PH, Reed JC, Laine J, Rivard N. MEK/ERK signaling pathway regulates the expression of Bcl-2, Bcl-X(L), and Mcl-1 and promotes survival of human pancreatic cancer cells. J Cell Biochem 2000;79:355–69.
41. Paus R, Cotsarelis G. The biology of hair follicles. N Engl J Med 1999;341:491–7.
42. Krimpenfort P, Quon KC, Mooi WJ, Loonstra A, Berns A. Loss of p16Ink4a confers susceptibility to metastatic melanoma in mice. Nature 2001;413:83–6.
43. Bardeesy N, Bastian BC, Hezel A, Pinkel D, DePinho RA, Chin L. Dual inactivation of RB and p53 pathways in RAS-induced melanomas. Mol Cell Biol 2001;21:2144–53.
44. Chin L, Pomerantz J, Polsky D, et al. Cooperative effects of INK4a and ras in melanoma susceptibility *in vivo*. Genes Dev 1997;11:2822–34.
45. Ackermann J, Frutschi M, Kaloulis K, McKee T, Trumpp A, Beermann F. Metastasizing melanoma formation caused by expression of activated N-RasQ61K on an INK4a-deficient background. Cancer Res 2005;65:4005–11.
46. You MJ, Castrillon DH, Bastian BC, et al. Genetic analysis of Pten and Ink4a/Arf interactions in the suppression of tumorigenesis in mice. Proc Natl Acad Sci U S A 2002;99:1455–60.
47. Sibilia M, Fleischmann A, Behrens A, et al. The EGF receptor provides an essential survival signal for SOS-dependent skin tumor development. Cell 2000;102:211–20.
48. Gille H, Downward J. Multiple ras effector pathways contribute to G(1) cell cycle progression. J Biol Chem 1999;274:22033–40.
49. Michaloglou C, Vredeveld LC, Soengas MS, et al. BRAFE600-associated senescence-like cell cycle arrest of human naevi. Nature 2005;436:720–4.
50. Chen Z, Trotman LC, Shaffer D, et al. Crucial role of p53-dependent cellular senescence in suppression of Pten-deficient tumorigenesis. Nature 2005;436:725–30.

Pten Deficiency in Melanocytes Results in Resistance to Hair Graying and Susceptibility to Carcinogen-Induced Melanomagenesis

Tae Inoue-Narita, Koichi Hamada, Takehiko Sasaki, et al.

Cancer Res 2008;68:5760-5768.